Gastric Cancer (2021) 24:85–102
https://doi.org/10.1007/s10120-020-01099-9

ORIGINAL ARTICLE

RP11-323N12.5 promotes the malignancy and immunosuppression of human gastric cancer by increasing *YAP1* transcription

Jianjun Wang[1] · Feng Huang[1] · Yaxiang Shi[2] · Qinghui Zhang[1] · Song Xu[1] · Yongliang Yao[1] · Runqiu Jiang[3,4,5]

Received: 26 December 2019 / Accepted: 12 June 2020 / Published online: 4 July 2020

Abstract

Background YAP1 is a core protein of the Hippo signaling pathway and is associated with malignancy and immunosuppression. In the present study, we discovered a novel lncRNA, *RP11-323N12.5*, with tumor promotion and immunosuppression activities through enhancing transcription of YAP1.

Methods *RP11-323N12.5* was identified using GEPIA. Its expression levels and their relationship with clinical features were investigated using clinical samples. The regulation of YAP1 transcription by *RP11-323N12.5* was investigated in both GC and T cells, the tumor and immunosuppression promotion roles of *RP11-323N12.5* were explored i*n vitro* and in vivo.

Results *RP11-323N12.5* was the most up-regulated lncRNA in human GC, based on data from the TCGA database. Its transcription was significantly positively correlated with YAP1 transcription, YAP1 downstream gene expression which contribute to tumor growth and immunosuppression. *RP11-323N12.5* promoted YAP1 transcription by binding to c-MYC in the *YAP1* promoter region. Meanwhile, transcription of *RP11-323N12.5* was also regulated by YAP1/TAZ/TEADs activation in GC cells. *RP11-323N12.5* had tumor- and immnosuppression-promoting effects by enhancing YAP1 downstream genes in GC cells. Excessive *RP11-323N12.5* was also observed in tumor-infiltrating leukocytes (TILs), which may be exosome-derived and also be related to enhanced Treg differentiation as a result *YAP1* up-regulation. Moreover, *RP11-323N12.5* promoted tumor growth and immunosuppression via YAP1 up-regulation in vivo.

Conclusions *RP11-323N12.5* was the most up-regulated lncRNA in human GC and it promoted *YAP1* transcription by binding to c-MYC within the *YAP1* promoter in both GC and T cells. *RP11-323N12.5* is an ideal therapeutic target in human GC due to its tumor-promoting and immunosuppression characteristics.

Keywords *RP11-323N12.5* · YAP1 · Hippo signaling · Immunosuppression · Gastric cancer

Abbreviations

GC	Gastric cancer
lncRNA	Long non-coding RNA
TILs	Tumor infiltrating leukocytes
TCGA	The Cancer Genome Atlas Program
GTEx	The Genotype-Tissue Expression
STAD	Stomach adenocarcinoma

Jianjun Wang, Feng Huang and Yaxiang Shi have contributed equally to this work.

Electronic supplementary material The online version of this article (https://doi.org/10.1007/s10120-020-01099-9) contains supplementary material, which is available to authorized users.

✉ Yongliang Yao
yyl313@163.com

✉ Runqiu Jiang
jiangrq@nju.edu.cn

[1] Department of Clinical Laboratory, Kunshan First People's Hospital, Affiliated To Jiangsu University, Kunshan 215300, People's Republic of China

[2] Department of Gastroenterology, Zhenjiang Hospital Affiliated to Nanjing University of Chinese Medicine, Zhenjiang 212000, People's Republic of China

[3] Department of Hepatobiliary Surgery, The Affiliated Drum Tower Hospital of Nanjing University Medical School, Nanjing 210093, Jiangsu, People's Republic of China

[4] Medical School of Nanjing University, Nanjing, People's Republic of China

[5] Jiangsu Laboratory of Molecular Medicine, Nanjing University, Nanjing 210093, People's Republic of China

LPA	Lysophosphatidic acid
ISH	In situ hybridization
ChIRP	Chromatin isolation by RNA purification assay

Background

Long noncoding RNAs (lncRNAs) have gained widespread attention by biological and medical researchers recently. However, decades ago, lncRNAs were termed "junk DNA" due to its transposons, pseudogenes, and simple repeats, which make up approximately 70% of the human genome [1, 2]. With the evolution of high-throughput RNA sequencing and genetic modification techniques, more functional lncRNAs have been investigated in various human diseases, especially in malignancies, such as lung cancer, gastric cancer, liver cancer, colorectal cancer, and leukemia [3–6]. The functional mechanisms of lncRNAs are varied and include chromatin remodeling and chromatin interactions, as well as acting as enhancers, promoters, or introns of other genes; pseudogenes; or natural antisense transcripts [7, 8]. In addition, lncRNAs may also host one or more small RNAs within their transcriptional units. Besides their function within tumor cells, tumor-derived lncRNAs also modulate the tumor microenvironment via exosomes, switching tumor immunity from anti-cancer to pro-cancer by targeting signaling pathways in different immunocytes [9–12].

Hippo signaling is one of the tumor- and tumor immunosuppression-related signaling pathways that was first discovered in *Drosophila melanogaster* through genetic mosaic screens [13, 14]. The Hippo signaling pathway consists of the NDR family protein kinase, Warts (Wts); the WW domain–containing protein, Salvador (Sav); the Ste20-like protein kinase, Hippo (Hpo); and the adaptor protein Mob as tumor suppressor (Mats) [13, 14]. Dysregulation of Hippo pathway components has been demonstrated in many cancers [15]. Besides its promotion of cell proliferation, dysregulation of Hippo signaling has also been shown to regulate many normal biological and disease processes, including survival, metabolism, stemness, angiogenesis, invasion, and immunosuppression [15, 16]. In addition to classical stimuli of Hippo signaling, many studies have reported its regulation by lncRNAs [17, 18]. Therefore, an investigation of the diagnostic value and mechanisms of lncRNAs that target Hippo signaling is warranted.

GEPIA is an online tool for analyzing RNA sequencing data from 9736 tumors and 8587 normal samples from the Cancer Genome Atlas Program (TCGA) and the Genotype-Tissue Expression (GTEx) project, using a standard processing pipeline [19]. Using this tool, we obtained 104 most differentially expressed transcripts between human gastric cancer and normal stomach tissues. Among these transcripts, we found that *RP11-323N12.5* was the most significantly up-regulated lncRNA. Correlation analysis indicated that it was related to tumor growth and immunosuppression genes within the Hippo signaling pathway. In the present study, the clinical diagnostic value and functional mechanisms of *RP11-323N12.5* were explored.

Materials and methods

TCGA database analysis and bioinformatics analysis

We used GEPIA, an online TCGA and GTEx analysis tool, to identify differentially expressed genes in the stomach adenocarcinoma (STAD) subset. TRANSFAC (www.gene-regulation.com) and PROM (https://alggen.lsi.upc.es/) were used to predict the potential binding sites in the promoter regions of *YAP1* or *RP11-323N12.5* (1000 bp upstream flanking sequence from the transcription start site).

Patients

This hospital-based case–control study included 67 GC patients. All subjects were recruited from the First People's Hospital of Kunshan, affiliated with Jiangsu University, between January 2017 and December 2018. All patients underwent surgery for primary GC and subjects with a previous history of cancer or chemotherapy were excluded. This study was approved by the Ethics Review Board of the First People's Hospital of Kunshan (KSL-2017017) and all patients provided written informed consent.

Cell lines and reagents

Human GC cell lines, including MKN45 and MGC-803, were purchased from the American Type Culture Collection (Manassas, VA, USA). Cells were cultured in Dulbecco's modified Eagle's medium (Gibco, Waltham, MA, USA), supplemented with 10% fetal bovine serum (FBS; Invitrogen, Carlsbad, CA, USA) and maintained at 37 °C in a humidified atmosphere containing 5% CO_2. Lysophosphatidic acid (LPA) was purchased from ENZO (BML-LP100-0025; Farmingdale, NY, USA) and an shRNA targeting YAP was purchased from Santa Cruz Biotechnology (sc-38637-V; Dallas, TX, USA). Positive clones were obtained using a puromycin screen.

Real-time PCR

Total RNA was isolated from GC tissues and cell lines using TRIzol reagent (Invitrogen, 15596026). Gene expression was assessed using a SYBR green-based real-time PCR method (AceQ Universal SYBR qPCR Master Mix, Vazyme,

Nanjing, China, Q511-02). The primers used in this study are listed in Supplementary Table 1.

Multicolor immunohistochemistry, immunofluorescence, and in situ hybridization

For multicolor staining, we processed slides strictly according to the instructions of the Opal 4-Anti-Rabbit Automation IHC kit (NEL830001KT; AKOYA Biosciences, Marlborough, MA, USA). Slides were incubated at 4 °C overnight with primary anti-YAP1 (#4912; Cell Signaling Technology, Danvers, MA, USA), anti-Survivin (ab76424; Abcam, Cambridge, UK) anti-human CD4 (ab181724, Abcam), anti-mouse CD4 (ab183685, Abcam), anti-COX2 (ab15191, Abcam), anti-human Foxp3 (ab20034, Abcam), and anti-mouse Foxp3 antibodies (ab75763, Abcam) and then photographed using a digital microscope camera (Nikon, Tokyo, Japan).

In situ hybridization (ISH) was performed using a Boster ISH kit (Boster, Wuhan, China). Cells were fixed and permeabilized using methanol and protease to allow biotin-labeled probes to access the cells. Cells were treated with 30% H_2O_2 in ddH_2O, at a ratio of 1:10, for 5 min, after which pepsase, diluted in 3% citric acid, was applied for 20 s. The second fixation was performed using 1% paraformaldehyde/0.1 M PBS. Next, the cells were incubated with pre-hybridization solution at 40 °C for 2 h and then with lncRNA target probes at 30 °C overnight, followed by two washes with 2× saline sodium citrate. After blocking, a biotin-labeled anti-digoxin antibody was added and cells were incubated for 60 min. The following sequence was used for the *RP11-323N12.5* probe: ctcctgcttgggggcgccgcgccgc.

Western blotting

For western blotting, proteins were extracted from cultured cells using RIPA buffer containing phenylmethanesulfonylfluoride (Beyotime, Nantong, China). An equal amount of protein per sample (100 μg) was separated by 7.5%/12.5% sodium dodecyl sulfate–polyacrylamide gel electrophoresis and transferred to a polyvinylidene fluoride membrane. The following primary polyclonal antibodies were used: anti-YAP1 (#4912, Cell Signaling Technology), anti-phospho(S127)-YAP1 (#13008, Cell Signaling Technology), anti-Survivin (ab76424, Abcam), anti-MMP9 (ab219372, Abcam), and anti-COX2 (ab15191, Abcam). HRP-conjugated anti-rabbit secondary antibodies were used (Abcam). The blots were developed using ECL reagent (WBKLS0500; Merck Millipore, Burlington, MA, USA). An equal amount of protein loading in each lane was confirmed using an anti-β-Actin antibody (ab8226, Abcam). ImageJ software was used to quantify the integrated density of the protein bands.

Luciferase gene reporter assay

The promoter region of the *YAP1* gene containing wild-type (WT) or mutant (MU) potential target sites for c-MYC, as well as the promoter region of the *RP11-323N12.5* gene containing wild-type or mutant binding sites for TEAD1, were designed and synthesized by Genescript, Co. (Nanjing, China) and inserted into the pGL4 Vector (Promega, Madison, WI, USA). For luciferase assays, MKN45, MGC803, and Jurkat cells were transfected with pGL4-YAP1 WT pro or pGL4-YAP1 c-MYC MU pro, pGL4-RP11-323N12.5 WT pro or pGL-4-RP11-323N12.5 TEAD1 MU pro, or control vector, using Lipofectamine 2000 (11668019, ThermoFisher Scientific, Waltham, MA, USA). LPA-treated cells were harvested 48 h after transfection and a luciferase assay was performed using a Dual-Luciferase® Reporter Assay System (E1910, Promega, Madison WI,), according to the manufacturer's protocol.

Chromatin isolation by RNA purification assay (ChIRP)

Chromatin isolation by RNA purification (ChIRP) assays were performed using an EZ- Magna ChIRP RNA Interactome Kit (17-10495, Millipore). The sequence of the *RP11-323N12.5* probe was GGGCGTTGGAGGCCTGC. Isolated RNA was used for qRT-PCR analysis to quantify the enrichment of chromatin. The qRT-PCR primer sequences used in this study were as follows: *YAP1* promoter: 5′-AATGAG TTTCACTGAGGGAT-3′ (forward) and 5′-CAAAACAAG CAATGTGAGGT-3′ (reverse).

CCK8 cell proliferation, cell colony formation, migration, and invasion assays

A CCK-8 assay kit (CK04-11, Dojindo, Kumamoto, Japan) was used to detect cell proliferation, according to the manufacturer's protocol. Cells were seeded into 96-well plates (500 cells/well in 100 μL of medium) and 10 μL of CCK-8 solution was added to each well at the same time each day for each time-point. After incubation for 2 h at 37 °C, the absorbance (450 nm) of each well was measured.

For cell colony formation assays, GC cells were plated in 6-well plates, at a density of 500 cells/well, and incubated for 2 weeks. Proliferating colonies were fixed with 75% alcohol and stained with crystal violet. Colonies containing ≥ 50 cells were counted under a microscope. All procedures were performed in triplicate.

For migration and invasion assays, cells were placed into the upper chamber of a transwell plate (8-μm pore size; Millipore), which was coated with (invasion assay) or without (migration assay) a Matrigel mix (BD Biosciences, San Jose, CA, USA), according to the manufacturer's protocol. After

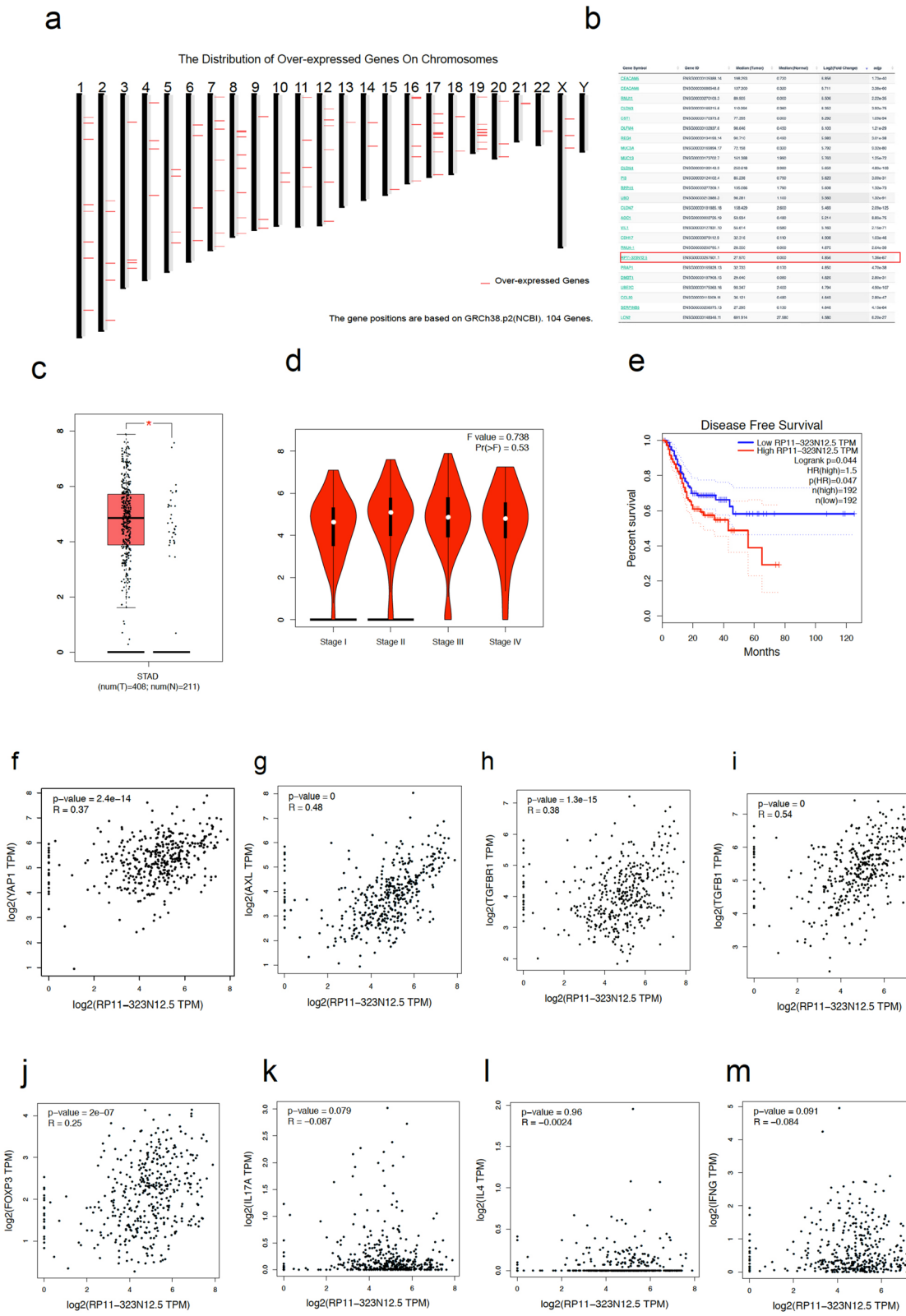
a
The Distribution of Over-expressed Genes On Chromosomes
1 2 3 4 5 6 7 8 9 10 11 12 13 14 15 16 17 18 19 20 21 22 X Y
Over-expressed Genes
The gene positions are based on GRCh38.p2(NCBI). 104 Genes.
b
c
STAD
(num(T)=408; num(N)=211)
d
F value = 0.738
Pr(>F) = 0.53
Stage I
Stage II
Stage III
Stage IV
e
Disease Free Survival
Low RP11−323N12.5 TPM
High RP11−323N12.5 TPM
Logrank p=0.044
HR(high)=1.5
p(HR)=0.047
n(high)=192
n(low)=192
Percent survival
Months
f
p−value = 2.4e−14
R = 0.37
log2(YAP1 TPM)
log2(RP11−323N12.5 TPM)
g
p−value = 0
R = 0.48
log2(AXL TPM)
log2(RP11−323N12.5 TPM)
h
p−value = 1.3e−15
R = 0.38
log2(TGFBR1 TPM)
log2(RP11−323N12.5 TPM)
i
p−value = 0
R = 0.54
log2(TGFB1 TPM)
log2(RP11−323N12.5 TPM)
j
p−value = 2e−07
R = 0.25
log2(FOXP3 TPM)
log2(RP11−323N12.5 TPM)
k
p−value = 0.079
R = −0.087
log2(IL17A TPM)
log2(RP11−323N12.5 TPM)
l
p−value = 0.96
R = −0.0024
log2(IL4 TPM)
log2(RP11−323N12.5 TPM)
m
p−value = 0.091
R = −0.084
log2(IFNG TPM)
log2(RP11−323N12.5 TPM)

◂**Fig. 1** *RP11-323N12.5* was the most up-regulated lncRNA in human gastric cancer associated with immunosuppression in the TCGA database. **a** The chromosomal distribution of over-expressed genes in human gastric cancer (GC). **b** A list of the top 25 up-regulated genes in human GC. **c** Comparison of *RP11-323N12.5* transcription in human GC ($n=408$) vs. adjacent normal tissues ($n=211$). **d** Transcription of *RP11-323N12.5* in different stages of human GC. **e** Survival analysis evaluating the association of *RP11-323N12.5* with disease-free survival of post-surgery GC patients. **f**–**m** Linear correlation analysis of *RP11-323N12.5* expression and *YAP1*, *AXL*, *TGFBR1*, *TGFB1*, *FOXP3*, *IL17A*, *IL4*, or *IFNg*

incubation for 24 h, the cells located on the upper membrane of the transwell chambers were removed with cotton wool, while cells that had migrated or invaded through the membrane were fixed with methanol for 10 min and stained with 0.1% crystal violet for 30 min at 37 °C. Cells in three randomly selected microscopic fields were counted for each group. Experiments were independently repeated three times.

ELISA

The secretion of PGE2 and CXCL15 into the supernatant of MKN45 and MGC-803 cells, *RP11-323N12.5*-overexpressing cells, and *RP11-323N12.5* + *YAP1* shRNA-transfected cells was measured using ELISA kits (ab133021 for PGE2, ab234567 for CXCL15; Abcam).

Treg cell differentiation and flow cytometric analysis

Various genetically modified Jurkat cells were obtained for the in vitro stimulation of Treg cell polarization. For the in vitro generation of Treg cells, Jurkat cells were stimulated with recombined human TGF-β (1 ng/mL; Peprotech, Rocky Hill, NJ, USA) for 7 days. Dead cells were excluded based on staining with a live/dead fixable dye. Thereafter, cells were fixed, permeabilized with IntraPrep reagent (BD Pharmingen, San Jose, CA, USA), and then stained with fluorochrome-conjugated antibodies against CD4 (20 µL per test, 555346), CD25 (20 µL per test, 555432), or Foxp3 (20 µL per test, 560082, BD Pharmingen). Data were acquired on a BD FACSVerse™ flow cytometer (BD Pharmingen).

Tumor-infiltrating leukocyte isolation

Fresh tissue–infiltrating lymphocytes were obtained as described previously [20]. Briefly, GC tissue specimens were cut into small pieces and digested in RPMI 1640. Dissociated cells were filtered through a 75 µm cell strainer and separated by Ficoll centrifugation. The mononuclear cells were then washed and resuspended in RPMI 1640, supplemented with 10% FBS (Gibco, Waltham, MA, USA). T cells were purified using anti-CD3 magnetic Dynabeads (Invitrogen Life Technologies, CA, USA) according to manufacturer's instruction.

Subcutaneous tumorigenesis assay

For subcutaneous tumorigenesis assays, tumor cells were injected subcutaneously in mice (2×10^6 cells/100 µl per flank containing 1×10^6 GC tumor cells and 1×10^6 peripheral mono-nuclear blood cells obtained from non-GC healthy volunteers) [20]. Four weeks after injection, the mice were euthanized. The tumor volume was calculated using the formula (width$^2\times$length)/2. The tumor tissues were then harvested for further analysis.

Statistical analysis

Data are presented as mean ± SD. Chi square tests and a two-tailed Student's *t* test analysis of variances were used to evaluate statistical differences in demographic and clinical characteristics. All in vitro expression experiments were repeated at least three times, each with triplicate samples. Pearson's correlation analysis was used to analyze the relationship between associated factors. Statistical analyses were performed using STATA 9.2 (StataCorp, College Station, TX, USA) and presented using Prism software (GraphPad, San Diego, CA, USA). In all cases, $P<0.05$ was considered significant.

Results

RP11-323N12.5 is the most overexpressed lncRNA in human gastric cancer, based on the TCGA data base

Based on the newly developed interactive web server, GEPIA [19], we found 3746 significantly up-regulated genes in stomach adenocarcinomas (STADs) compared to their paired normal tissues ($n=36$) using an ANOVA to analyze TCGA data. The chromosomal distribution of the top 104 differentially expressed genes is presented in Fig. 1a. The top 25 up-regulated genes are listed in Fig. 1b. *RP11-323N12.5* was found to be the most significantly up-regulated lncRNA in human GC tissues (Gene ID ENSG00000267601.1), with a median expression of 27.970 in tumors and 0.000 in normal tissues, with an adjusted *P* value 1.36e-67 (Fig. 1b). *RP11-323N12.5* is an anti-sense non-coding RNA located on chr17:78855478–78855844, with a transcript of 367 bp.

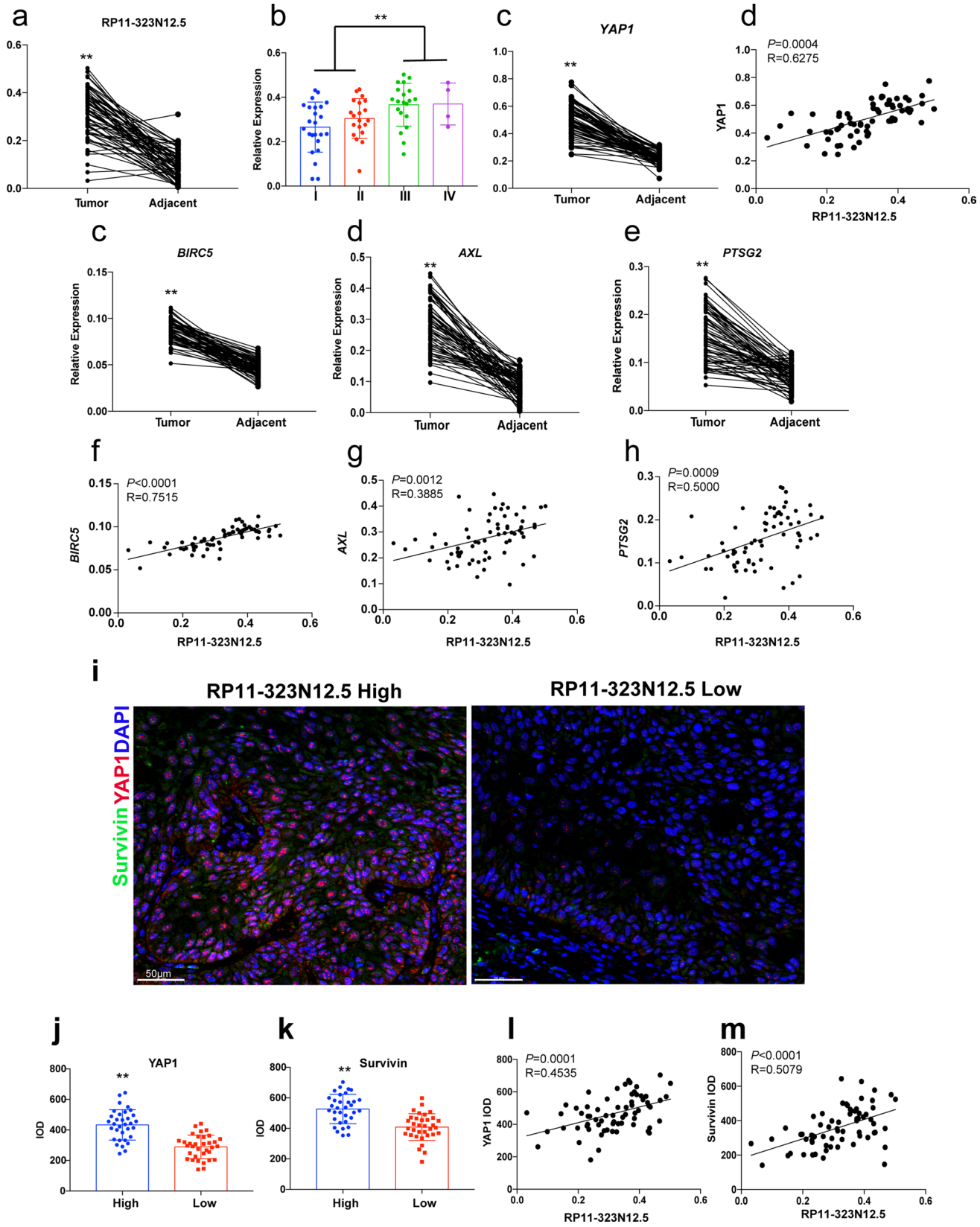
a
RP11-323N12.5
**
Tumor
Adjacent
b
**
Relative Expression
I
II
III
IV
c
YAP1
**
Tumor
Adjacent
d
P=0.0004
R=0.6275
YAP1
RP11-323N12.5
c
BIRC5
**
Relative Expression
Tumor
Adjacent
d
AXL
**
Relative Expression
Tumor
Adjacent
e
PTSG2
**
Relative Expression
Tumor
Adjacent
f
P<0.0001
R=0.7515
BIRC5
RP11-323N12.5
g
P=0.0012
R=0.3885
AXL
RP11-323N12.5
h
P=0.0009
R=0.5000
PTSG2
RP11-323N12.5
i
RP11-323N12.5 High
RP11-323N12.5 Low
Survivin YAP1 DAPI
50μm
j
YAP1
**
IOD
High
Low
k
Survivin
**
IOD
High
Low
l
P=0.0001
R=0.4535
YAP1 IOD
RP11-323N12.5
m
P<0.0001
R=0.5079
Survivin IOD
RP11-323N12.5

◂**Fig. 2** *RP11-323N12.5* was over-expressed in human GC tissues and was associated with the dysregulation of Hippo signaling. **a** Transcription of *RP11-323N12.5* in paired human GC and adjacent normal stomach tissues ($n=67$). **b** *RP11-323N12.5* expression at different stages of human GC. **c** Transcription of *YAP1* in paired human GC and adjacent normal stomach tissues ($n=67$). **d** Linear correlation analysis of *RP11-323N12.5* and YAP1 in human GC. **c**–**e** Transcription of *BIRC5*, *AXL*, and *PTSG2* in paired human GC and adjacent normal stomach tissues ($n=67$). **f**–**h** Linear correlation analysis of *RP11-323N12.5* and *BIRC5*, *AXL*, or *PTSG2* in human GC. **i** Representative figures of immunofluorescence (IF) staining of YAP1 and Survivin in human GC tissues with high and low levels of *RP11-323N12.5* expression. **j**, **k** Integrated optical intensity (IOD) analysis of YAP1 and Survivin protein expression in human GC tissues with high ($n=33$) and low ($n=34$) levels of *RP11-323N12.5* expression. **l**, **m** Linear correlation analysis of *RP11-323N12.5* and YAP1 or Survivin in human GC with high ($n=33$) and low ($n=34$) levels of *RP11-323N12.5* expression. Each experiment was performed in triplicate. Data are presented as the mean ± SEM and were analyzed by Student's *t* test ($^{**}P<0.01$)

Moreover, using a one-way ANOVA to analyze samples from the GTEx database, we found that *RP11-323N12.5* was also overexpressed in human GC tissues compared to normal tissues (GC $n=408$ vs. normal $n=211$, Fig. 1c). We found that *RP11-323N12.5* expression levels were significantly higher in advanced GC (TMN Stage I–II vs. Stage III, IV; Fig. 1d). Survival analysis showed that high *RP11-323N12.5* expression was significantly correlated with disease-free survival ($P=0.047$), but not with overall survival of post-surgery GC patients (Fig. 1e).

Through pathway enrichment analysis between *RP11-323N12.5*-high and *RP11-323N12.5*-low GC samples ($n=408$), we found that *RP11-323N12.5* expression was significantly related to Hippo signaling (data not shown). Furthermore, we confirmed this correlation by investigating the correlation between *RP11-323N12.5* and components of the Hippo signaling pathway and its downstream genes. These results indicated that *RP11-323N12.5* expression levels were significantly positively correlated with *YAP1*, *AXL*, and *TGFBR1* expression levels (Fig. 1f–h). Since, the inactivation of Hippo signaling is significantly associated with a suppressive tumor microenvironment (TME) in human solid tumors, we also investigated the correlation between *RP11-323N12.5* expression and the expression of genes representing different types of T helper cells. We found that *RP11-323N12.5* was significantly correlated with *FOXP3* and *TGFB1* expression (Fig. 1i, j), which implied that *RP11-323N12.5* was associated with Treg cells, but not Th1, Th2, or Th17 cells in the TME of human GC (Fig. 1k–m).

RP11-323N12.5 was associated with YAP1 expression in human GC

To confirm the overexpression of *RP11-323N12.5* in human GC, we collected 67 paired human GC and para-tumor tissues. We found that *RP11-323N12.5* was overexpressed in GC tissues compared to paired normal tissue (Fig. 2a). Moreover, *RP11-323N12.5* expression levels were also significantly higher in advanced stage GC (stage III–IV) compared to early stage GC (stage I–II, Fig. 2b). The transcription levels of *YAP1* were also determined by real-time PCR in 67 paired GC and normal tissues. Similar to previously published results [19], *YAP1* was found to be overexpressed in GC tissues and its expression levels were positively correlated with *RP11-323N12.5* expression levels ($P=0.0004$, $r=0.6275$). Moreover, we found that the downstream genes of Hippo signaling, *BIRC5*, *AXL*, and *PTSG2* were overexpressed in GC tissues (Fig. 2c, d, e) and their expression levels were also positively correlated with *RP11-323N12.5* expression levels in human GC tissues (*BIRC5* vs. *RP11-323N12.5*: $r=0.7515$, $P<0.0001$; *AXL* vs. *RP11-323N12.5*: $r=0.3885$, $P=0.0012$; and *PTSG2* vs. *RP11-323N12.5*: $r=0.5000$, $P=0.0009$; Fig. 2f, g, h).

We also detected the protein expression of YAP1 and the downstream, protein, Survivin, in human GC tissues by immunofluorescence staining, in two groups according to *RP11-323N12.5* expression (*RP11-323N12.5*-high, $n=33$ and *RP11-323N12.5*-low, $n=34$). We found that YAP1 and Survivin levels were higher in the *RP11-323N12.5*-high group than in the *RP11-323N12.5*-low group (Fig. 2i, j, k). YAP1 and Survivin protein levels were also positively correlated with *RP11-323N12.5* expression levels (*RP11-323N12.5* vs. YAP1: $P=0.0001$, $r=0.4535$; *RP11-323N12.5* vs. Survivin: $P<0.0001$, $r=0.5079$). Based on these data, we proposed that *RP11-323N12.5* may be associated with *YAP1* transcription and downstream gene activation.

RP11-323N12.5 and YAP1 promoted the transcription of each other by promoter binding in GC cells

Since clinical studies have indicated that *RP11-323N12.5* expression is positively correlated with *YAP1* transcription, we further investigated the detailed regulatory mechanisms of *RP11-323N12.5* and YAP1. Firstly, we overexpressed and knocked down *RP11-323N12.5* expression in the human GC cell lines, MKN45 and MCG803, respectively. We found that the changes in *YAP1* transcription were synchronized to *RP11-323N12.5* expression (Fig. 3a). We also investigated

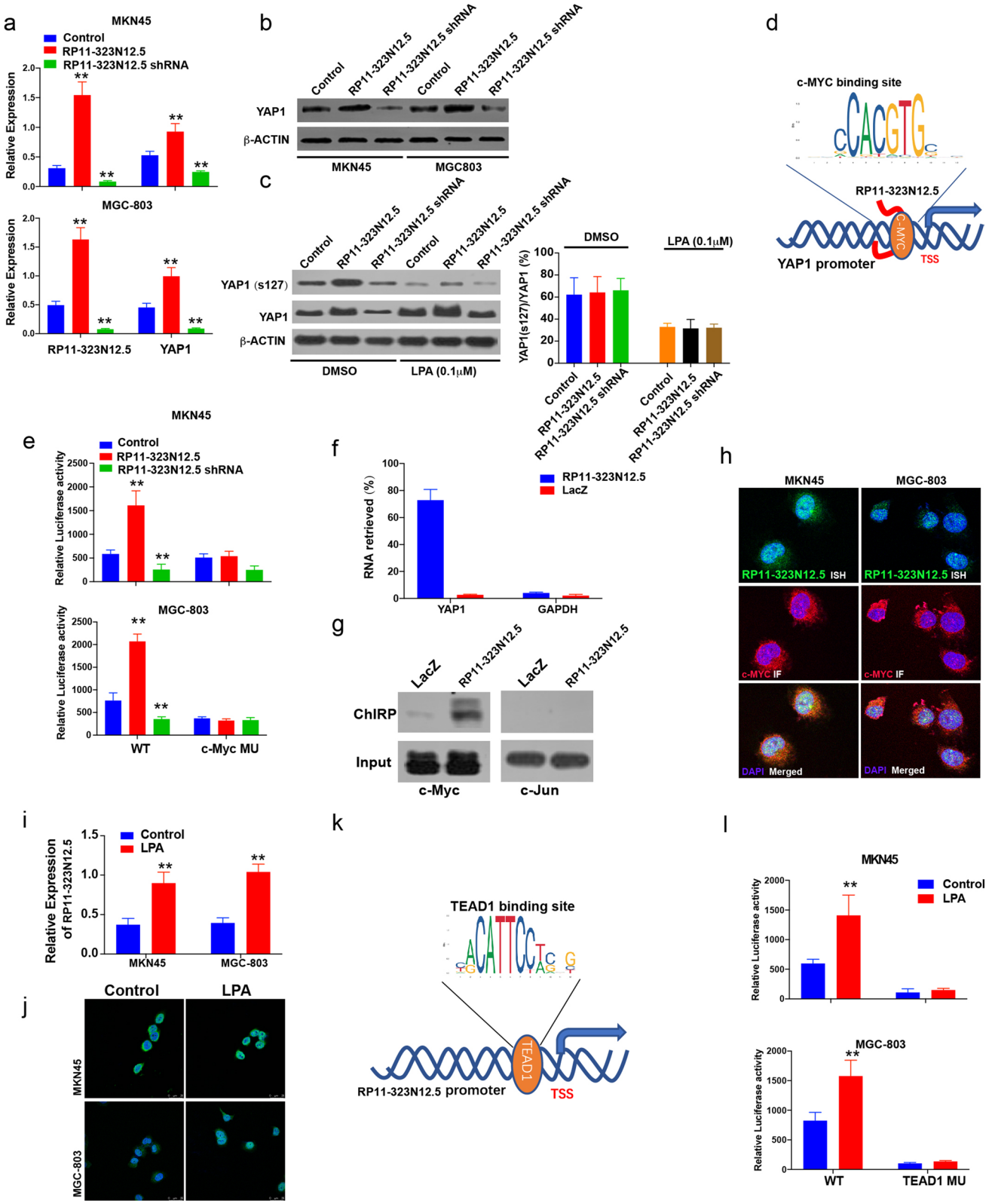
a
MKN45
Control
RP11-323N12.5
RP11-323N12.5 shRNA
Relative Expression
MGC-803
RP11-323N12.5
YAP1
b
Control
RP11-323N12.5
RP11-323N12.5 shRNA
YAP1
β-ACTIN
MKN45
MGC803
c
YAP1 (s127)
YAP1
β-ACTIN
DMSO
LPA (0.1μM)
YAP1(s127)/YAP1 (%)
d
c-MYC binding site
RP11-323N12.5
c-MYC
YAP1 promoter
TSS
e
MKN45
Relative Luciferase activity
MGC-803
WT
c-Myc MU
f
RNA retrieved (%)
YAP1
GAPDH
g
LacZ
ChIRP
Input
c-Myc
c-Jun
h
MKN45
MGC-803
RP11-323N12.5 ISH
c-MYC IF
DAPI
Merged
i
Relative Expression of RP11-323N12.5
LPA
j
k
TEAD1 binding site
TEAD1
RP11-323N12.5 promoter
TSS
l
TEAD1 MU

◂**Fig. 3** *RP11-323N12.5* and YAP1 promoted the transcription of each other by promoter binding in GC cells. **a** The transcription of *RP11-323N12.5* and *YAP1* in MKN45 and MGC-803 cells with different treatments. **b** Expression of YAP1 in MKN45 and MGC-803 cells with different treatments, using β-actin as an internal control. **c** Western blotting analysis of the levels of phosphorylated (S127) and total YAP1 in MKN45 cells after treatment with 0.1 μM LPA or DMSO (control) for 6 h. **d** Schematic diagram of the mechanism whereby *RP11-323N12.5* promotes *YAP1* transcription by binding to c-MYC in the *YAP1* gene promoter. **e** Luciferase gene reporter assay of *YAP1* promoter activity in MKN45 and MGC-803 cells with different treatments. **f** RNA retrieval rate in chromatin isolation by RNA purification (ChIRP) assays, using probes targeting *RP11-323N12.5* and LacZ (control). **g** c-MYC and c-Jun protein detection in proteins obtained from the ChIRP assay. **h** Co-localization assay determining the distribution and expression of *RP11-323N12.5* (by ISH) and c-MYC (by IF) in the human GC cell lines, MKN45 and MGC-803. **i**, **j** *RP11-323N12.5* transcription was measured by real-time PCR and ISH in MKN45 and MGC-803 cells, 6 h after treatment with DMSO (control) or LPA (0.1 μM). **k** Schematic diagram of the promotion of *RP11-323N12.5* transcription by YAP/TAZ/TEADs. **l** Luciferase gene reporter assay of *RP11-323N12.5* promoter activity in MKN45 and MGC-803 cells treated with LPA (0.1 μm) or DMSO (1 h after treatment). Each experiment was performed in triplicate. Data are presented as the mean ± SEM and were analyzed by Student's *t* test ($^{**}P < 0.01$)

YAP1, which showed a similar trend to its transcription levels (Fig. 3b). However, the expression of *RP11-323N12.5* had no effect on YAP1 activation. The YAP1 activator, LPA (0.1 μM) can decrease the phosphorylation of the S127 residue of YAP1 and increase total YAP1 protein levels, but *RP11-323N12.5* had no effect on the ratio of YAP1(S127)/YAP1 (Fig. 3c). These results implied that *RP11-323N12.5* can regulate *YAP1* transcription, but not YAP1 activation.

We screened for potential binding between *RP11-323N12.5* and transcription factors (TFs) at the *YAP1* gene promoter and found that c-Myc was the TF linking *RP11-323N12.5* and *YAP1* transcription (*YAP1* promoter region [−216 bp to −211 bp], Fig. 3d). Based on this prediction, we constructed WT and c-Myc binding site mutation (c-Myc MU) *YAP1* promoters and found that *RP11-323N12.5* overexpression increased and RP11-323 N12.5 knockdown decreased *YAP1* promoter activity. However, *RP11-323N12.5* expression had almost no effect on the *YAP1* promoter with the c-Myc binding site mutated (Fig. 3e). We also used a ChIRP assay to confirm the binding of *RP11-323N12.5* to c-MYC. Specific primers targeting c-Myc bound to the promoter region retrieved a DNA sequence pull downed by the *RP11-323N12.5* probe. Western blotting analysis further confirmed the existence of c-Myc protein in the *RP11-323N12.5* probe precipitate (Fig. 3f, g). Lastly, we investigated the location of *RP11-323N12.5* and c-Myc in MKN-45 and MGC 803 cells. ISH results indicated that *RP11-323N12.5* was located mainly in the nucleus and we found that c-Myc and *RP11-323N12.5* co-localized in the nuclei of both MKN-45 and MCG 803 cells (Fig. 3h).

Since *RP11-323N12.5* was overexpressed in GC and its transcription was positively correlated with Hippo inactivation, based on our clinical investigation and data from the TCGA database, we next investigated whether YAP1 activation could promote *RP11-323N12.5* transcription. Firstly, LAP-induced YAP1 activation was shown to significantly increase *RP11-323N12.5* transcription in both MKN45 and MCG 803 cells, as determined by both real-time PCR and ISH analyses (Fig. 3i, j). When we queried the promoter region of *RP11-323N12.5*, we found that a TEAS1 binding site existed within this region (Fig. 3k). Therefore, we performed a luciferase gene reporter assay and found that LAP did not increase *RP11-323N12.5* promoter activity when the TEAD1 binding site was mutated (Fig. 3l). These results indicated that *RP11-323N12.5* and YAP1 can promote each other's expression in human GC.

RP11-323N12.5 promoted GC cell proliferation and invasion, as well as immunosuppression, by increasing YAP1 expression

Since *RP11-323N12.5* and YAP1 can promote each other's expression in human GC, we investigated the mechanisms of this phenomenon in vitro. Three types of cell lines were constructed including WT cells; cells overexpressing *RP11-323N12.5* (*RP11-323N12.5*); and cells overexpressing *RP11-323N12.5*, with YAP1 knocked down (*RP11-323N12.5* + YAP1 shRNA). Cell proliferation was monitored using CCK8 assay and colony formation assays. We found that *RP11-323N12.5* promoted the proliferation of both MKN45 and MGC803 cells; however, this effect was mainly dependent on YAP1 expression (Fig. 4a, b). *RP11-323N12.5* markedly increased the migration and invasion ability of both GC cell lines. When YAP1 was knocked down by a specific shRNA, cell migration and invasion decreased to levels significantly less than those observed in WT cells (Fig. 4c). These data implied that *RP11-323N12.5* is a YAP1-dependent oncogene. These oncogenic effects may be carried out by up-regulating Survivin, MMP9, and AXL, which were up-regulated by *RP11-323N12.5* overexpression and down-regulated by knocking down YAP1 (Fig. 4d, e).

Since previous studies have shown that inactivation of Hippo signaling is significantly related to immunosuppression [21, 22] and data from TCGA also implied that *RP11-323N12.5* was significantly correlated with Treg cell-related immunosuppression, we analyzed genes downstream of YAP1 and immunosuppression-related genes, including *PSTG2*, *CSF1*, *CXCL15*, and *CSF3*. We found that *RP11-323N12.5* significantly promoted the expression of these genes in a YAP1-dependent manner (Fig. 4d, e).

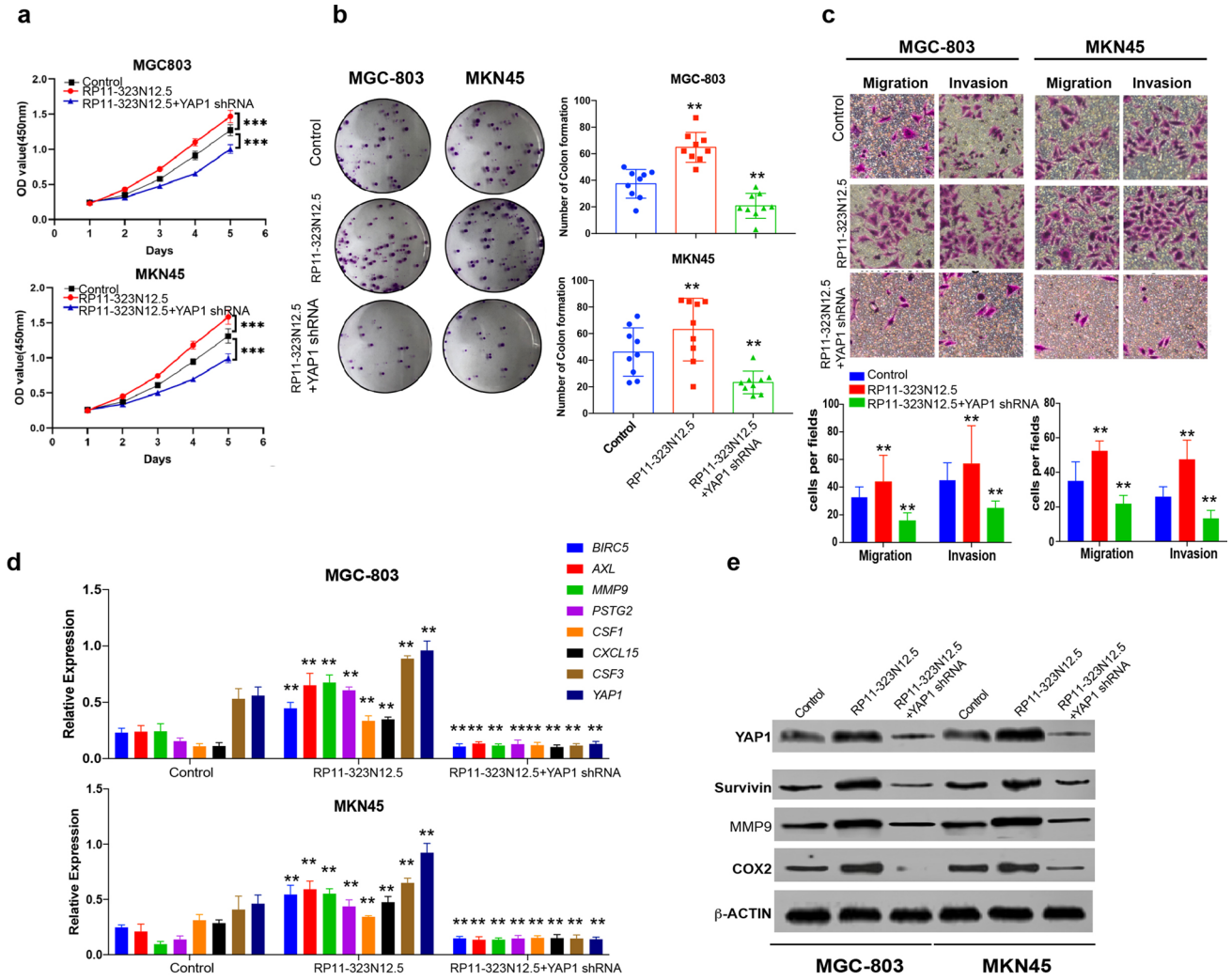

Fig. 4 *RP11-323N12.5* promoted cell proliferation, migration, and invasion by up-regulating YAP1. The human GC cell lines, MGC-803 and MKN45, underwent various treatments and cell proliferation (**a**), colony formation (**b**), and cell migration and invasion ability (**c**) were then determined. **d** Gene expression was measured by real-time PCR in MGC-803 and MKN45 cells with different treatments. All of the tested genes are downstream of YAP1 activation. **e** The protein downstreams of YAP1 activation were measured by western blotting in MGC-803 and MKN45 cells with different treatments. Each experiment was performed in triplicate. Data are presented as the mean ± SEM and were analyzed by Student's *t* test ($^{**}P < 0.01$)

RP11-323N12.5 was related to Treg cell- and MDSC-related immunosuppression in the human GC tumor microenvironment

Based on in vitro studies, we found that *RP11-323N12.5* may be related to Treg cell differentiation via cytokine secretion. We also investigated the relationship between *RP11-323N12.5* expression and Treg cell distribution by multicolor immunohistochemistry (IHC). We found that in tissues with high levels of *RP11-323N12.5* expression, the percentage of Treg cells was much higher than in tissues with low levels of *RP11-323N12.5* expression. This was accompanied by higher levels of COX2 expression, which are reported to induce Tregs by increasing PGE2 expression in cancer (Fig. 5a–c). Moreover, we found a positive correlation between *RP11-323N12.5* expression levels and the percentage of Tregs and COX2 expression in human GC (Fig. 5d, e). Next, we found more Tregs and MDSCs in GC tissues with high levels of *RP11-323N12.5* expression than in those with low levels of *RP11-323N12.5*

expression (Figs. 5f, g, S1a, b). Furthermore, we found that serum PGE2 and CXCL15 levels were markedly higher in GC patients with high levels of *RP11-323N12.5*-expression (Fig. 5h, i).

We next investigated PGE2 and CXCL15 secretion by human GC cell lines after various treatments. We found that *RP11-323N12.5* promote the secretion of these proteins in a YAP1-dependent manner (Fig. 5j, k). We also co-cultured human T cells, isolated from six non-GC individuals, with MKN45 cells, after various treatments, for 7 days. We found that Treg cell differentiation was significantly increased by co-culture with *RP11-323N12.5*-overexpressing MKN45 cells, but this effect was inhibited by YAP1 depletion in MKN45 cells (Fig. 5l).

RP11-323N12.5 promoted Treg cell differentiation by enhancing *YAP1* transcription in T cells

Since we observed that *RP11-323N12.5* was related to Treg cell-induced immunosuppression by tumor-derived secretion, we next investigated whether endogenous *RP11-323N12.5* could promote Treg cell differentiation. Firstly, we investigated YAP1 protein expression in CD4+ T cells using multicolor IHC. We found that T cell expression levels of YAP1 were higher in GC tissues expressing high levels of *RP11-323N12.5* compared to those expressing low levels of *RP11-323N12.5*. Moreover, *RP11-323N12.5* levels were also significantly positively corelated with the expression levels of these genes (Fig. 6c). These results indicated that endogenous *RP11-323N12.5* in T cells was not only related to tumor cell *RP11-323N12.5* expression, but also related to Treg cell differentiation. TILs were isolated from human GC tissues and *RP11-323N12.5* levels were found to be significantly higher in GC tissues expressing high levels of *RP11-323N12.5* than in those with low levels of *RP11-323N12.5* expression. Treg cell-related genes, including *YAP1*, *FOXP3*, *TGFBR2,* and *IL10* were all expressed at significantly higher levels in T cells isolated from tissues expressing high levels of *RP11-323N12.5* compared to those expressing low levels of *RP11-323N12.5*. We wondered that RP11-323N12.5 whether can promote YAP1 transcription in T cells.

We used Jurkat cells, a human T cell line, to further investigate this mechanism. Firstly, we found that overexpression of *RP11-323N12.5* in Jurkat cells enhanced Treg cell differentiation and this effect was YAP1 activation dependent (Fig. 6f). Both mRNA and protein expression of YAP1 were up-regulated by *RP11-323N12.5* (Fig. S2a, b). Next, we used a ChIRP assay to show that *RP11-323N12.5* promoted *YAP1* transcription by binding to c-MYC, specifically in the promoter region of the *YAP1* gene (Fig. 6g). Similar results were seen in luciferase gene reporter assays, indicating that *YAP1* promoter activity can be significantly increased by *RP11-323N12.5* in a c-MYC binding-dependent manner, since promoter activity was fully restored once the c-MYC binding site was mutated (Fig. 6h). However, using both luciferase gene reporter assays and real-time PCR, we found that YAP1 activation had no effect on *RP11-323N12.5* transcription in Jurkat cells (Fig. S2c, d). Next, we measured *RP11-323N12.5* levels in both GC patient serum samples and in cell culture supernatants. We found that *RP11-323N12.5* can be detected in the exosomes and its quantity varied according to *RP11-323N12.5* expression levels within tumor cells (Fig. 6i, j, k). Furthermore, we co-cultured *RP11-323N12.5* shRNA-transfected Jurkat cells with human GC cells showing different levels of *RP11-323N12.5* expression. The result indicated that *RP11-323N12.5* can transfer into Jurkat cells by exosome delivery (Figs. 6j, k, S2e). Therefore, we concluded that the high levels of *RP11-323N12.5* expression in T cells were exosome derived.

RP11-323N12.5 promoted tumor growth and immunosuppression via YAP1 up-regulation in vivo

To investigate the pro-cancer and pro-immunosuppressive effects of *RP11-323N12.5* in vivo, we performed a subcutaneous tumorigenesis assay using wild-type MKN45 cells; MKN45 cells overexpressing *RP11-323N12.5*; and MKN45 cells overexpressing *RP11-323N12.5*, with YAP1 knockdown. Simultaneously, the human mono-nuclear peripheral blood cells mainly containing T cells and monocytes were implanted subcutaneously with the tumor cells. *RP11-323N12.5* significantly promoted tumor growth, but this effect was completely inhibited by YAP1 knockdown in vivo (Fig. 7a). The TME derived from different tumor cells was also investigated by multicolor IHC staining of YAP1, Foxp3, and Cd4. We found that YAP1 was up-regulated by *RP11-323N12.5* in vivo and the number of infiltrating Treg cells increased in tumors derived from *RP11-323N12.5*-overexpressing MKN45 cells. However the number of infiltrating Treg cells decreased significantly when YAP1 was knocked down in MKN45-derived tumor tissue (Fig. 7b–d). Furthermore, TILs were isolated from the tumors and the numbers of both Treg cells and MDSCs were found to be increased in *RP11-323N12.5*-overexpressing tumors. However, their numbers decreased markedly when YAP1 expression was silenced in *RP11-323N12.5*-overexpressing tumor tissues (Fig. 7e, f).

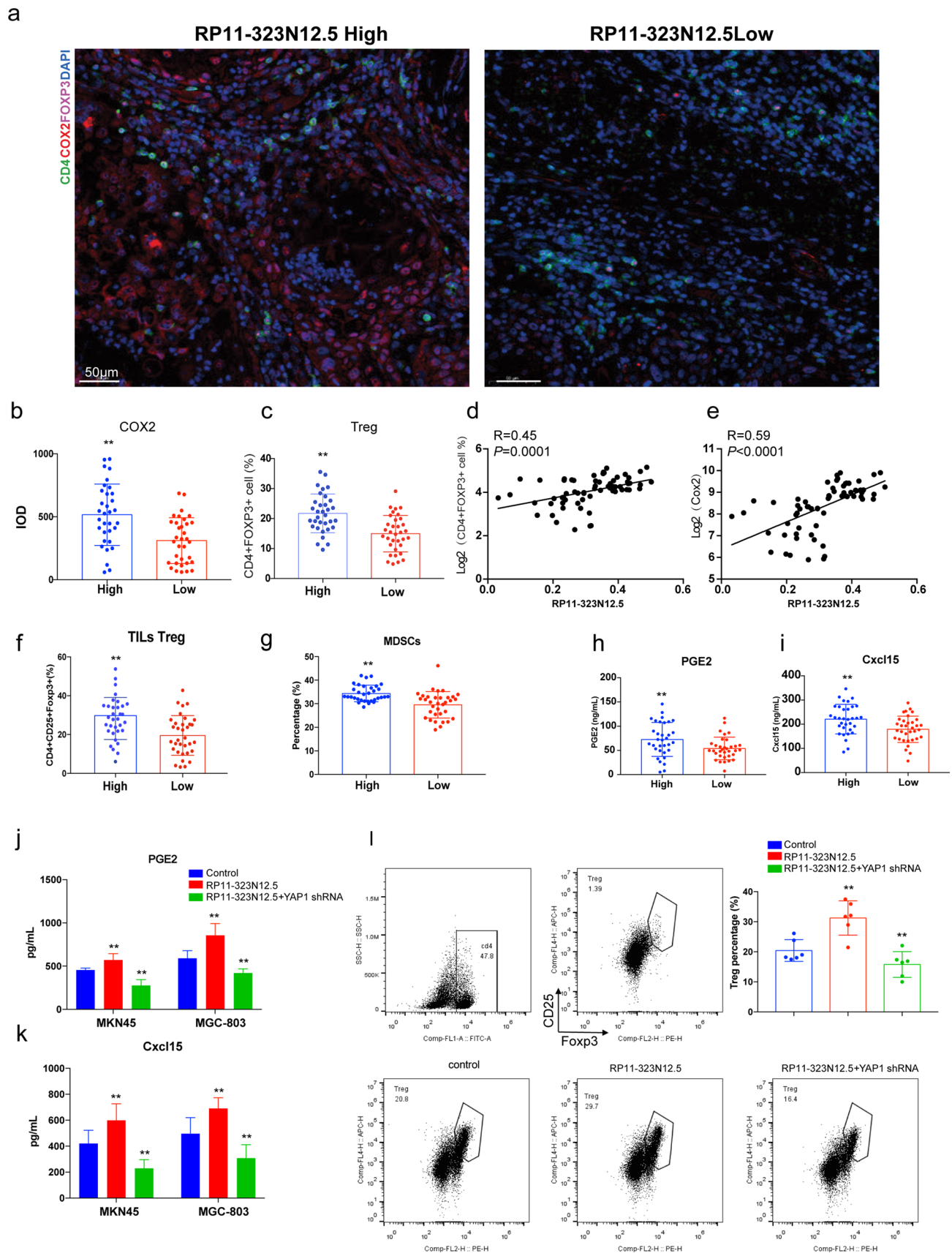
a
RP11-323N12.5 High
RP11-323N12.5Low
CD4 COX2 FOXP3 DAPI
50μm
b
COX2
IOD
High
Low
c
Treg
CD4+FOXP3+ cell (%)
d
R=0.45
P=0.0001
Log2 (CD4+FOXP3+ cell %)
RP11-323N12.5
e
R=0.59
P<0.0001
Log2 (Cox2)
f
TILs Treg
CD4+CD25+Foxp3+(%)
g
MDSCs
Percentage (%)
h
PGE2
PGE2 (ng/mL)
i
Cxcl15
Cxcl15 (ng/mL)
j
PGE2
Control
RP11-323N12.5
RP11-323N12.5+YAP1 shRNA
pg/mL
MKN45
MGC-803
k
Cxcl15
l
Treg 1.39
CD25
Foxp3
Treg percentage (%)
control
RP11-323N12.5
RP11-323N12.5+YAP1 shRNA
Treg 20.8
Treg 29.7
Treg 16.4

◂**Fig. 5** *RP11-323N12.5* was involved in Treg cell-related immunosuppression in the human GC tumor microenvironment. **a** Representative figures of multicolor staining of CD4, COX2, and FOXP3 in human GC tissues with high and low levels of *RP11-323N12.5* expression. **b**, **c** Integrated optical density (IOD) values of COX2 and CD4 + FOXP3 + cell percentage (CD4 + FOXP3 + /CD4) in human GC tissues with high ($n = 33$) and low ($n = 34$) levels of *RP11-323N12.5* expression. **d**, **e** Linear correlation analysis of *RP11-323N12.5* and CD4 + FOXP3 percentage (log2) or COX2 IOD values (log2) in human GC. **f**, **g** Tumor-infiltrating leukocytes were isolated from human GC tissues with high ($n = 33$) and low ($n = 34$) *RP11-323N12.5* expression levels and the percentages of Treg cells (CD4 + CD25 + FOXP3 +) and MDSCs (CD11b + CD33 +) were determined by flow cytometry. **h**, **i** The concentrations of PGE2 and Cxcl15 were determined in the serum of patients with high ($n = 33$) and low ($n = 34$) *RP11-323N12.5* expression levels. **j**, **k** The levels of PGE2 and Cxcl15 secreted from MKN45 and MGC-803 cells after different treatments were determined by ELISA. **l** The human T cell isolated from six non-GC persons was co-cultured with MKN45 cells treated with TGF-β (1 ng/mL) for 7 days and the percentage of Treg cells (CD4 + CD25 + FOXP3 +) was determined by flow cytometry. Each experiment was performed in triplicate. Data are presented as the mean ± SEM and were analyzed by Student's *t* test ($^{**}P < 0.01$)

In summary, in the present study, we used data from the TCGA database to identify *RP11-323N12.5* as the most differentially expressed lncRNA between human GC and normal tissue. *RP11-323N12.5* was shown to promote the transcriptional activation of *YAP1* in GC cells and further promote immunosuppression by Treg cell differentiation and MDSCs infiltration via a YAP1 activation dependent manner (Fig. 8).

Discussion

In the present study, we found that a novel lncRNA, *RP11-323N12.5*, contributed to the overexpression of YAP1 in human GC. Although it is a controversial notion that YAP overexpression alone is related to the development of GC, several studies have identified YAP1 as an oncoprotein in the stomach. In normal and proliferating normal gastric epithelium, low or moderate levels of YAP1 expression are detected, whereas significantly elevated YAP1 levels are consistently observed in both primary and metastatic GC [23, 24]. YAP1 expression is strongly positively correlated with lymphatic metastasis and shortened overall survival time, indicating that YAP may be used as an independent prognostic marker for GC [25–27]. Moreover, knockdown of YAP markedly suppresses cell proliferation, colony formation, and metastasis in GC cell lines, both in vitro and in vivo [28–30]. Besides the overexpression of YAP1, dysregulation of other genes within the Hippo signaling pathway have been reported more frequently. These include NF2, MST1/2, LATS1/2, and RASSF1A, which can increase the transcriptional activity of YAP1/TAZ/TEADs in human GC. Hippo signaling is also associated with immunosuppression [21]. On one hand, the activation of YAP1 signaling in tumor cells induces immunosuppression by up-regulating various cytokines, chemokines, and other molecules associated with the recruitment of M2 macrophages, Tregs, and MDSCs and by inhibition the infiltration and activity of NK cells and effector T-cells. On the other hand, YAP1 overexpression in immune cells facilitates immunosuppressive cell differentiation and proliferation [21]. For example, YAP1 induces the differentiation of naïve T-cells to Treg cells by up-regulating TGFBR2 [31]. In stromal cells, YAP1 promotes the transcription of myofibroblast marker genes, such as *α-SMA*, *CYR61*, and *CTGF* to activate cancer-associated fibroblasts (CAFs) in breast cancer. Activated YAP1 then recruits CAFs, MDSCs, and Tregs, leading to the impairment of CD8+ T-cells [32]. Our data confirmed this mechanism. We found that *RP11-323N12.5* not only promoted the malignancy of human GC, but also promoted immunosuppression by upregulating YAP1 activation-related cytokines. We found that once YAP1 levels decreased in GC cells, the *RP11-323N12.5*-induced immunosuppressive TME was totally reversed and the percentage of Treg cells and MDSCs decreased markedly.

For decades, the "on" state of the Hippo pathway has been regarded as a tumor suppressor pathway, due to its inhibition of proliferation and promotion of apoptosis [15, 16, 28, 30]. Dysregulation of the Hippo pathway is associated with a broad spectrum of cancers, mainly due to the core protein, YAP-1 [15]. YAP1 has been identified as an oncoprotein, associated with many different types of cancer [15]. Zhang et al. showed that YAP expression is markedly elevated in clinical hepatocellular carcinoma (HCC) samples and that YAP is a key driver gene in hepatitis B virus X protein (HBx)-induced hepatocarcinogenesis in a CREB-dependent manner. YAP may serve as a novel target in HBV-associated HCC therapy [33]. Moreover, there are several clinical studies showing that YAP protein is associated with the progression and prognosis of human GC. For example, Zhang et al. first reported that YAP is strongly expressed

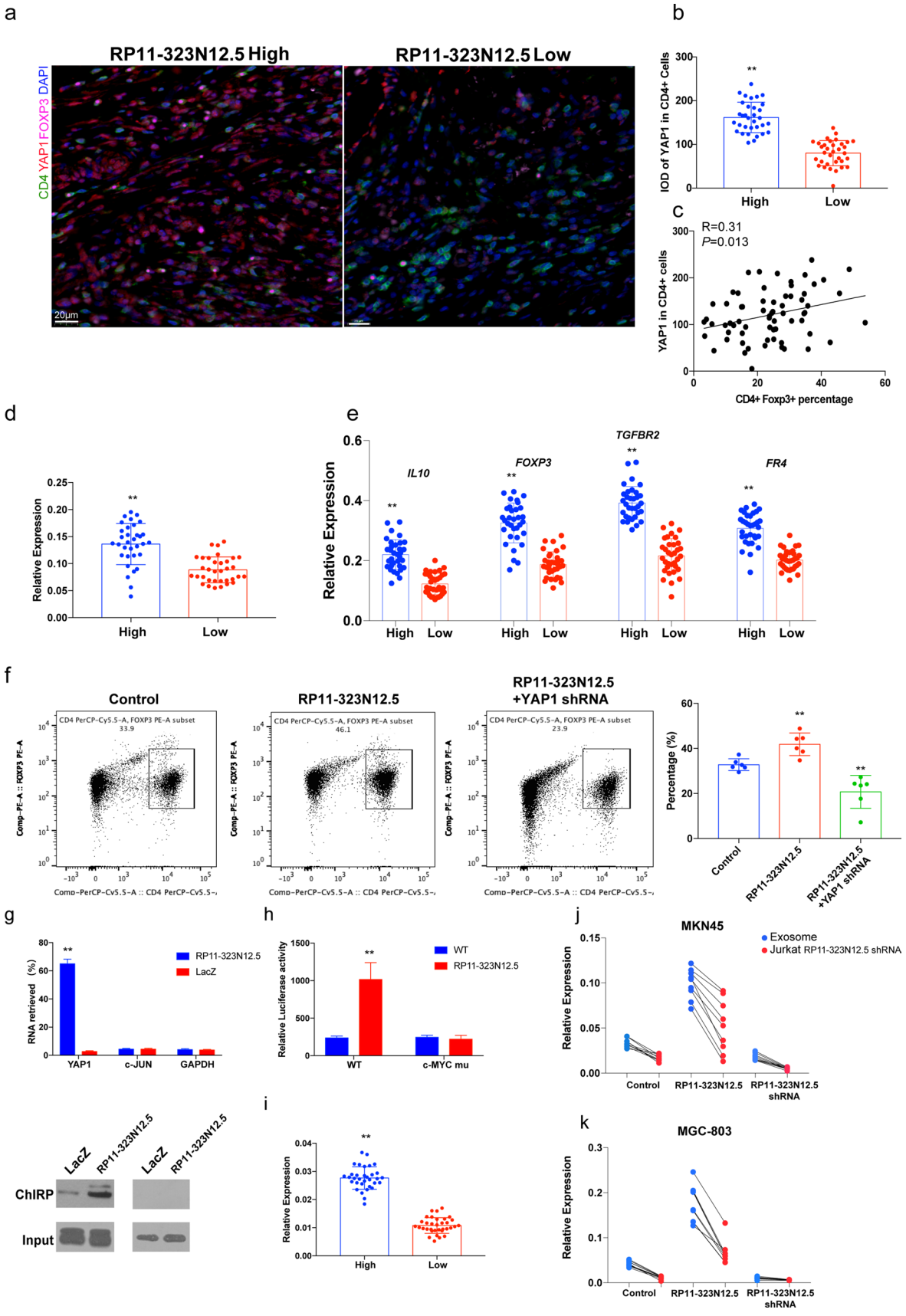
a
RP11-323N12.5 High
RP11-323N12.5 Low
CD4 YAP1 FOXP3 DAPI
20μm
b
IOD of YAP1 in CD4+ Cells
High
Low
c
R=0.31
P=0.013
YAP1 in CD4+ cells
CD4+ Foxp3+ percentage
d
Relative Expression
High
Low
e
Relative Expression
IL10
FOXP3
TGFBR2
FR4
High
Low
f
Control
RP11-323N12.5
RP11-323N12.5 +YAP1 shRNA
Percentage (%)
g
RNA retrieved (%)
RP11-323N12.5
LacZ
YAP1
c-JUN
GAPDH
h
Relative Luciferase activity
WT
RP11-323N12.5
c-MYC mu
i
ChIRP
Input
LacZ
RP11-323N12.5
Relative Expression
j
MKN45
Exosome
Jurkat RP11-323N12.5 shRNA
Relative Expression
Control
RP11-323N12.5
RP11-323N12.5 shRNA
k
MGC-803
Relative Expression
Control
RP11-323N12.5
RP11-323N12.5 shRNA

◂**Fig. 6** *RP11-323N12.5* promoted Treg cell differentiation by enhancing *YAP1* transcription in T cells. **a** Representative figures of multicolor staining of CD4, YAP1, and FOXP3 in human GC tissues with high and low levels of *RP11-323N12.5* expression. **b** Integrated optical density (IOD) values of YAP1 expression in CD4+ T cells in human GC with high ($n=33$) and low ($n=34$) levels of *RP11-323N12.5* expression. **c** Linear correlation analysis of YAP1 IOD values in CD4+ T cells and the percentage of CD4 + FOXP3 cells in human GC. **d** The transcription of *RP11-323N12.5* was measured by real-time PCR in tumor-infiltrating lymphocytes (TILs) isolated from human GC tissues with high ($n=33$) and low ($n=34$) levels of *RP11-323N12.5* expression. **e** The transcription of *IL10*, *FOXP3*, *TGFBR2*, and *FR4* was determined in TILs isolated from human GC tissues with high ($n=33$) and low ($n=34$) levels of *RP11-323N12.5* expression. **f** Jurkat cells with different levels of *RP11-323N12.5* expression were treated with TGF-β 1 ng/mL for 7 days and the percentage of Treg cells (CD4 + CD25 + FOXP3) was determined by flow cytometry. **g** ChIRP assays were performed in Jurkat cells using probes targeting *RP11-323N12.5* and LacZ (control). **h** Luciferase gene reporter assay of *YAP1* gene promoter activity in Jurkat cells with different levels of *RP11-323N12.5* expression. **i** Detection of *RP11-323N12.5* in serum exosomes of GC patients with high ($n=33$) and low ($n=34$) levels *RP11-323N12.5* expression. **j, k** The measurement of *RP11-323N12.5* in supernatant exosomes of cultured MKN45 and MGC-803 human GC cell lines and Jurkat cells with *RP11-323N12.5* knockdown. Each experiment was performed in triplicate. Data are presented as the mean ± SEM and were analyzed by Student's *t* test ($^{**}P<0.01$)

in gastric adenocarcinomas and that YAP knockdown may inhibit gastric cancer cell proliferation and metastasis [34]. Chol et al. showed that YAP and TAZ are oncogenic initiators and drivers in human GC, with MYC as the downstream effector [35].

Besides the protein-coding genes that regulate Hippo signaling, recently, a greater number of non-coding RNAs have been reported to modulate Hippo signaling. *MAYA*, a lncRNA, has been reported to mediate the methylation and upstream kinase activity of MST1/2 in Hippo signaling, which consequently, leads to the failure of LATS1 phosphorylation and YAP1 target gene activation in bone metastasis [36]. A recent study also identified a lncRNA, *BCAR4*, as a direct transcriptional target of YAP, involved in YAP-dependent glycolysis. Mechanistically, the long-term activation of YAP up-regulates the transcription of *BCAR4*, which, in turn, promotes the transcription of two glycolysis-related enzymes, HK2 and PFKFB3, through Hedgehog effector GLI2/p300 complex-mediated histone acetylation, marked by H3K27ac [37]. Similar to the lncRNAs, *MAYA* and *BCAR4*, *RP11-323N12.5* is also a Hippo signaling-associated lncRNA. However, *RP11-323N12.5* functions differently, in that it is an enhancer of *YAP1* transcription by binding to c-MYC, which is a transcriptional factor that regulates YAP1 [38].

Several studies have shown that lncRNAs can act as enhancers for certain genes by binding to DNA or protein. The lncRNA, *MAGI2-AS3*, prevents the development of HCC by recruiting KDM1A and promoting H3K4me2 demethylation of the *RACGAP1* gene promoter [39]. Chen et al. identified an exosome-derived lncRNA, termed lymph node metastasis-associated transcript 2 (*LNMAT2*), which stimulates human lymphatic endothelial cell (HLEC) tube formation and migration in vitro and enhances tumor lymphangiogenesis and LN metastasis in vivo. LNMAT2 was shown to be present at high levels in bladder cancer-derived exosomes by directly interacting with heterogeneous nuclear ribonucleoprotein A2B1 (hnRNPA2B1). Subsequently, exosomal LNMAT2 is internalized by HLECs and epigenetically up-regulates prospero homeobox 1 (PROX1) expression by the recruitment of hnRNPA2B1 and by increasing H3K4 trimethylation levels in the *PROX1* promoter, ultimately resulting in lymphangiogenesis and lymphatic metastasis [40].

Conclusion

In the present study, we identified the lncRNA, *RP11-323N12.5*, as the most significantly up-regulated lncRNA in human GC, based on data from the TCGA database. Mechanistically, *RP11-323N12.5* promoted *YAP1* transcription by binding to c-MYC in its promoter region. *RP11-323N12.5* also promoted malignancy and immunosuppression in a YAP1 activation-dependent manner. Moreover, *RP11-323N12.5* expression can be increased by YAP1/TAZ/TEADs. Therefore, *RP11-323N12.5* is a novel lncRNA contributing to the increased YAP1 expression seen in human GC.

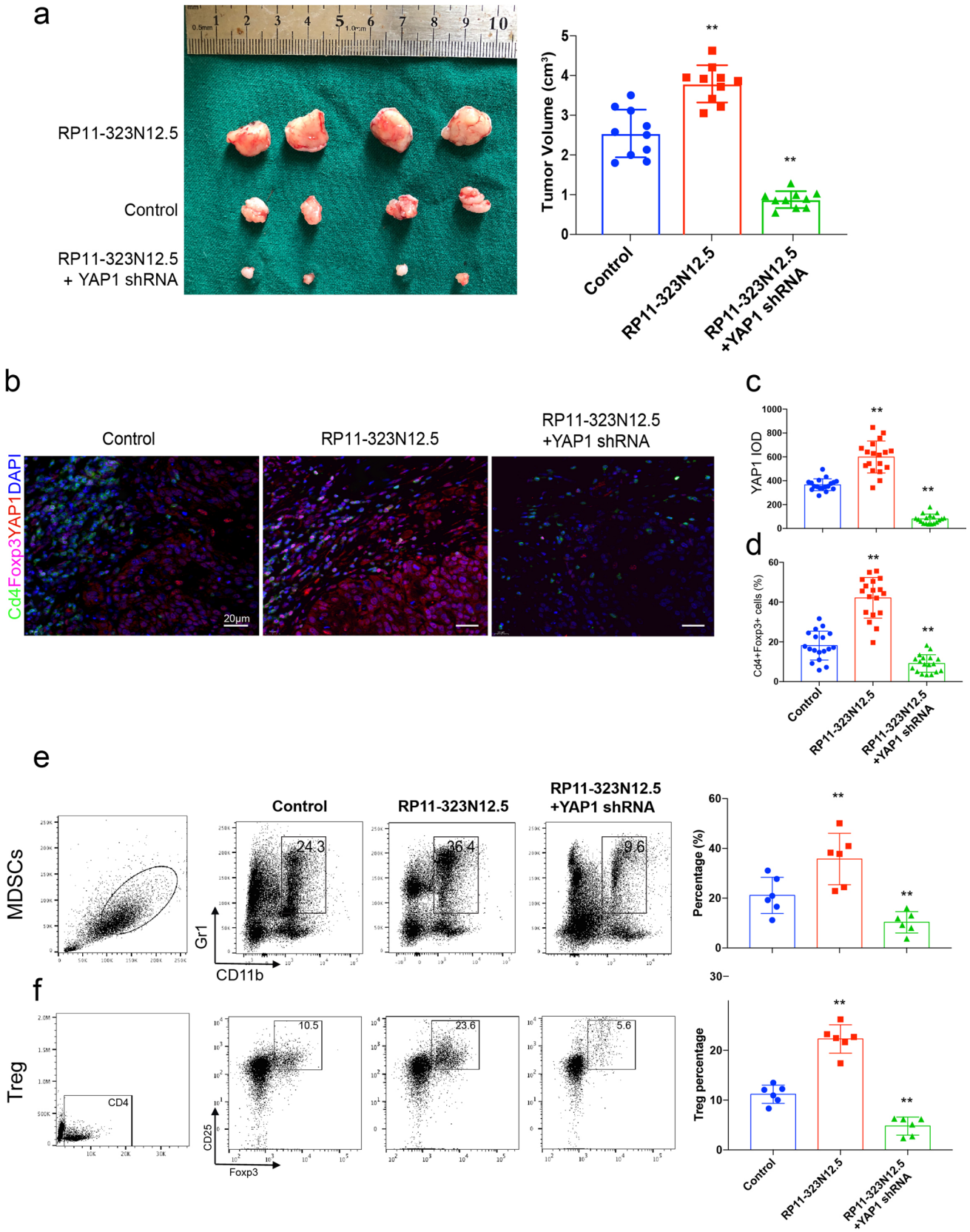
a
RP11-323N12.5
Control
RP11-323N12.5
+ YAP1 shRNA
Tumor Volume (cm³)
Control
RP11-323N12.5
RP11-323N12.5
+YAP1 shRNA
b
Control
RP11-323N12.5
RP11-323N12.5
+YAP1 shRNA
Cd4Foxp3YAP1DAPI
20μm
c
YAP1 IOD
d
Cd4+Foxp3+ cells (%)
e
MDSCs
Control
RP11-323N12.5
RP11-323N12.5
+YAP1 shRNA
24.3
36.4
9.6
Gr1
CD11b
Percentage (%)
f
Treg
CD4
10.5
23.6
5.6
CD25
Foxp3
Treg percentage

◂**Fig. 7** *RP11-323N12.5* promoted tumor growth and immunosuppression in vivo. **a** Subcutaneous tumorigenesis assay using MKN45 cells with different levels of gene expression, as indicated ($n=6$ per group, left panel). Comparison of tumor volume in all three groups (right panel). **b** Multicolor staining of YAP1, CD4, and Foxp3 in tumor tissues. **c**, **d** Comparison of YAP1 expression and CD4 + Foxp3 + cells within tumor tissues of all three groups. **e**, **f** Comparison of Treg cells and MSDCs within tumor-infiltrating lymphocytes isolated from tumor tissues of all three groups. Each experiment was performed in triplicate. Data are presented as the mean ± SEM and were analyzed by Student's *t* test ($^{**}P<0.01$)

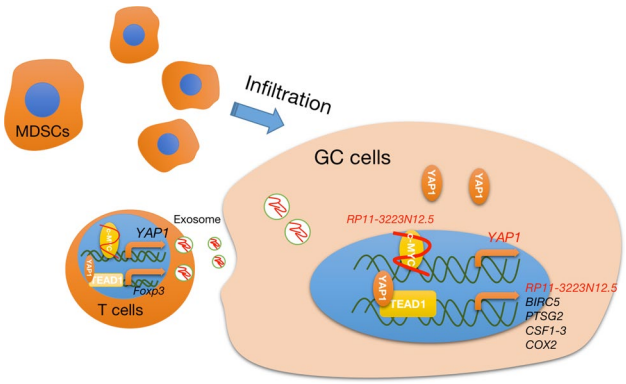

Fig. 8 Graphic summary of *RP11-323N12.5* promoted tumor growth and immunosuppression in human Gastric cancer

Author contributions Conception and design: JRQ and YYL. Collection and assembly of data: JJW, FH, SX, and YXS data analysis and interpretation: JJW and FH. Contribution of reagents, materials, and analysis tools wrote the paper: JJW, FH and QHZ. All authors read and approved the final manuscript.

Funding This work was supported by grants from the National Natural Science Foundation (Grant numbers: 81772262 to Y.Y., 81572370, 81772569 and 81972266 to R.J.).

Compliance with ethical standards

Conflict of interest The authors declared no competing interests.

Ethical approval Animal experiments were approved and performed in accordance with the institutional guidelines for animal care of animal ethics committee of the First People's Hospital of Kunshan (KSL-2017017). All institutional and national guidelines for the care and use of laboratory animals were followed.

Human and animal rights All procedures followed were in accordance with the ethical standards of the responsible committee on human experimentation (institutional and national) and with the Helsinki Declaration of 1964 and later versions.

Informed consent Informed consent to be included in the study, or the equivalent, was obtained from all patients.

References

1. Lee H, Zhang Z, Krause HM. Long noncoding RNAs and repetitive elements: junk or intimate evolutionary partners? Trends Genet. 2019;35(12):892–902.
2. Wang J, et al. ncRNA-Encoded peptides or proteins and cancer. Mol Ther. 2019;27(10):1718–25.
3. Wei L, et al. The emerging role of microRNAs and long noncoding RNAs in drug resistance of hepatocellular carcinoma. Mol Cancer. 2019;18(1):147.
4. Bermudez M, et al. LncRNAs as regulators of autophagy and drug resistance in colorectal cancer. Front Oncol. 2019;9:1008.
5. Hua JT, Chen S, He HH. Landscape of noncoding RNA in prostate cancer. Trends Genet. 2019;35(11):840–51.
6. Fattahi S, et al. LncRNAs as potential diagnostic and prognostic biomarkers in gastric cancer: a novel approach to personalized medicine. J Cell Physiol. 2019;235(4):3189–206.
7. Vafadar A, et al. Long non-coding RNAs: epigenetic regulators in cancer. Curr Pharm Des. 2019;25(33):3563–77.
8. Zhang L, et al. Long non-coding RNAs in ocular diseases: new and potential therapeutic targets. FEBS J. 2019;286(12):2261–72.
9. Botti G, et al. LncRNA HOTAIR in tumor microenvironment: what role? Int J Mol Sci. 2019;20(9):2279.
10. Feng W, et al. ncRNAs associated with drug resistance and the therapy of digestive system neoplasms. J Cell Physiol. 2019;234(11):19143–57.
11. Dong P, et al. Exploring lncRNA-mediated regulatory networks in endometrial cancer cells and the tumor microenvironment: advances and challenges. Cancers. 2019;11(2):234.
12. Lin YH, et al. Long non-coding RNAs as mediators of tumor microenvironment and liver cancer cell communication. Int J Mol Sci. 2018;19(12):3742.
13. Mia MM, Singh MK. The hippo signaling pathway in cardiac development and diseases. Front Cell Dev Biol. 2019;7:211.
14. Zhang S, Zhou D. Role of the transcriptional coactivators YAP/TAZ in liver cancer. Curr Opin Cell Biol. 2019;61:64–71.
15. Zheng Y, Pan D. The hippo signaling pathway in development and disease. Dev Cell. 2019;50(3):264–82.
16. Pan Z, et al. The emerging role of YAP/TAZ in tumor immunity. Mol Cancer Res. 2019;17(9):1777–866.
17. Lin X, et al. Super-enhancer-associated LncRNA UCA1 interacts directly with AMOT to activate YAP target genes in epithelial ovarian cancer. iScience. 2019;17:242–55.
18. Zhu Y, et al. The MRVI1-AS1/ATF3 signaling loop sensitizes nasopharyngeal cancer cells to paclitaxel by regulating the Hippo-TAZ pathway. Oncogene. 2019;38(32):6065–81.
19. Tang Z, et al. GEPIA: a web server for cancer and normal gene expression profiling and interactive analyses. Nucleic Acids Res. 2017;45(W1):W98–W102.
20. Jiang R, et al. Interleukin-22 promotes human hepatocellular carcinoma by activation of STAT3. Hepatology. 2011;54(3):900–9.
21. Shibata M, Ham K, Hoque MO. A time for YAP1: tumorigenesis, immunosuppression and targeted therapy. Int J Cancer. 2018;143(9):2133–44.
22. Ni X, et al. YAP is essential for treg-mediated suppression of antitumor immunity. Cancer Discov. 2018;8(8):1026–43.
23. Kim SH, et al. Activating hippo pathway via rassf1 by ursolic acid suppresses the tumorigenesis of gastric cancer. Int J Mol Sci. 2019;20(19):4709.
24. Kim E, et al. High yes-associated protein 1 with concomitant negative LATS1/2 expression is associated with poor prognosis of advanced gastric cancer. Pathology. 2019;51(3):261–7.
25. Nambara S, et al. Antitumor effects of the antiparasitic agent ivermectin via inhibition of yes-associated protein 1 expression in gastric cancer. Oncotarget. 2017;8(64):107666–77.

26. Han XY, et al. Expression of VGLL4 and YAP protein in gastric carcinoma tissues and tumor prognosis. Minerva Med. 2018;109(6):429–35.
27. Lee KW, et al. Development and validation of a six-gene recurrence risk score assay for gastric cancer. Clin Cancer Res. 2016;22(24):6228–355.
28. Sun D, et al. YAP1 enhances cell proliferation, migration, and invasion of gastric cancer in vitro and in vivo. Oncotarget. 2016;7(49):81062–76.
29. Li P, et al. Elevated expression of Nodal and YAP1 is associated with poor prognosis of gastric adenocarcinoma. J Cancer Res Clin Oncol. 2016;142(8):1765–73.
30. Kang W, et al. Yes-associated protein 1 exhibits oncogenic property in gastric cancer and its nuclear accumulation associates with poor prognosis. Clin Cancer Res. 2011;17(8):2130–9.
31. Fan Y, et al. YAP-1 promotes tregs differentiation in hepatocellular carcinoma by enhancing TGFBR2 transcription. Cell Physiol Biochem. 2017;41(3):1189–98.
32. Zhang K, et al. Mechanical signals regulate and activate SNAIL1 protein to control the fibrogenic response of cancer-associated fibroblasts. J Cell Sci. 2016;129(10):1989–2002.
33. Zhang T, et al. Hepatitis B virus X protein modulates oncogene yes-associated protein by CREB to promote growth of hepatoma cells. Hepatology. 2012;56(6):2051–9.
34. Zhang J, et al. Expression of yes-associated protein in gastric adenocarcinoma and inhibitory effects of its knockdown on gastric cancer cell proliferation and metastasis. Int J Immunopathol Pharmacol. 2012;25(3):583–90.
35. Choi W, et al. YAP/TAZ initiates gastric tumorigenesis via upregulation of MYC. Cancer Res. 2018;78(12):3306–20.
36. Li C, et al. A ROR1-HER3-lncRNA signalling axis modulates the hippo-YAP pathway to regulate bone metastasis. Nat Cell Biol. 2017;19(2):106–19.
37. Zheng X, et al. LncRNA wires up Hippo and Hedgehog signaling to reprogramme glucose metabolism. EMBO J. 2017;36(22):3325–35.
38. Mo X, et al. AKT1, LKB1, and YAP1 revealed as MYC interactors with NanoLuc-based protein-fragment complementation assay. Mol Pharmacol. 2017;91(4):339–47.
39. Pu J, et al. lncRNA MAGI2-AS3 prevents the development of HCC via recruiting KDM1A and promoting H3K4me2 demethylation of the RACGAP1 promoter. Mol Ther Nucleic Acids. 2019;18:351–62.
40. Chen C, et al. Exosomal long noncoding RNA LNMAT2 promotes lymphatic metastasis in bladder cancer. J Clin Invest. 2020;130(1):404–21.